

Original Article

# Optimizing Relay Coordination in Radial Distribution Systems with Solar PV Integration

T. Kosaleswara Reddy<sup>1</sup>, T. Devaraju<sup>2</sup>, M. Vijayakumar<sup>3</sup>

<sup>1,3</sup>Department of EEE, Jawaharlal Nehru Technological University Anantapur, Andhra Pradesh, India.

<sup>2</sup>Department of EEE, Sree Vidyanikethan Engineering College, Andhra Pradesh, India.

<sup>2</sup>Corresponding Author : [devaraj@vidyanikethan.edu](mailto:devaraj@vidyanikethan.edu)

Received: 01 May 2024

Revised: 03 June 2024

Accepted: 01 July 2024

Published: 26 July 2024

**Abstract** - Relay coordination in radial distribution systems is crucial for ensuring efficient and reliable power distribution, especially with the integration of solar Photovoltaic (PV) systems. The operation of relay backup to enhance system protection and accommodate renewable energy sources is the focus of this research. Various relay coordination strategies are investigated using the IEEE-13 bus system as a testbed. Key aspects such as currents and time multiplier settings are considered to develop an effective coordination scheme. Additional complexity is introduced by the integration of solar PV systems due to bidirectional power flow and intermittent generation. The proposed coordination strategies are evaluated for their effectiveness in maintaining system stability and minimizing outage risks through validation with Mi-Power software. The findings contribute to the development of advanced relay coordination techniques tailored for modern distribution networks with renewable energy integration. Challenges are addressed, and system performance and reliability are optimized. This research provides insights into the critical aspects of relay coordination in radial distribution systems. The complexities introduced by solar PV systems are carefully considered, and strategies are developed to manage these challenges effectively. The IEEE-13 bus system serves as an ideal testbed for exploring various coordination schemes, and the use of Mi-Power software ensures robust validation of the proposed strategies.

**Keywords** - Coordination analysis, Protection schemes, Radial distribution system, Relay coordination, Solar PV system, Reliability.

## 1. Introduction

Optimizing relay coordination in radial distribution systems is a critical aspect of ensuring the reliable and efficient operation of electrical power systems. Radial distribution systems, characterized by their single-path configuration from the substation to the end consumers, are widely used due to their simplicity and cost-effectiveness. However, this configuration presents unique challenges in maintaining the selective coordination of protective devices, which is essential for minimizing the impact of faults and maintaining service continuity.

Relay coordination involves setting protective relays in such a way that they operate in a pre-defined sequence during fault conditions. This ensures that the protective device closest to the fault isolates the affected section, thereby minimizing disruptions to the larger network. Effective relay coordination is pivotal in radial systems to prevent unnecessary outages and equipment damage, enhance safety, and maintain the stability of the distribution network. One of the primary challenges in optimizing relay coordination in radial systems is achieving the right balance between sensitivity and selectivity. Relays

must be sensitive enough to detect faults quickly yet selective enough to ensure that only the faulted section is isolated. Several factors, including the type and setting of relays, network topology, and fault current levels, influence this balance. Modern techniques for optimizing relay coordination have evolved significantly, leveraging advancements in computational tools and optimization algorithms.

Traditional Time-Current Characteristic (TCC) curves, used to set relay operation times, are now augmented with intelligent systems that can dynamically adjust settings based on real-time network conditions. Techniques such as genetic algorithms, particle swarm optimization, and artificial neural networks have shown promise in addressing the complexities of relay coordination in radial distribution systems. Furthermore, the integration of Distributed Generation (DG) into radial networks introduces additional layers of complexity. DG sources can alter fault current levels and directions, complicating the relay coordination process. Advanced optimization techniques must, therefore, account for these changes to maintain effective protection schemes. The advent of smart grid technologies also offers new



opportunities for optimizing relay coordination. Smart grids enable enhanced communication and control capabilities, allowing for more precise and adaptive relay settings. This can significantly improve the responsiveness and reliability of protection systems in radial distribution networks [1-3].

The integration of solar photovoltaic systems into radial distribution systems has garnered significant attention due to its impact on fault currents. Radial distribution systems, typically characterized by a unidirectional flow of electricity from the substation to end-users, experience notable changes in operational dynamics when Solar PV systems are added. Solar PV systems, unlike conventional synchronous generators, contribute fault current differently due to their inverter-based design. Inverters, which convert the Direct Current (DC) output of PV panels into Alternating Current (AC), limit the fault current contribution to 1.1 to 1.2 times their rated output. This is considerably lower compared to synchronous generators, which can contribute fault currents up to 6 to 10 times their rated capacity [4].

The inclusion of Solar PV can lead to both positive and negative impacts on the protection schemes of radial distribution systems. Positively, the lower fault current contribution from PV inverters may reduce the thermal and mechanical stress on the system components during faults, potentially extending their operational life. However, this same characteristic can pose challenges to existing protection systems designed for higher fault currents. Traditional overcurrent protection devices may fail to detect and isolate faults effectively if the fault current contribution from the PV systems is insufficient to trigger the protection settings.

With significant penetration of Solar PV, radial systems, which are designed for unidirectional power flow, may experience bidirectional power flow. This can complicate fault detection and isolation. Additionally, during faults, there is a risk of unintentional islanding, where a section of the distribution network continues to be powered by the PV systems even when disconnected from the main grid. This scenario poses safety risks to maintenance personnel and can complicate the restoration process. Several strategies can mitigate the impact of Solar PV on fault currents in radial distribution systems.

Adaptive protection schemes, which adjust their settings based on the real-time operating conditions of the network, can enhance the detection and isolation of faults. Implementation of Fault Current Limiters (FCLs) can also help manage the fault current contributions from PV systems, ensuring they remain within the protective device's operating range. Furthermore, advanced inverter technologies, which can emulate the fault current characteristics of traditional generators, are being developed to improve compatibility with existing protection schemes [5-7]. Adaptive protection schemes are seen as a promising solution for distribution

networks with high IBR penetration. These schemes involve real-time adjustment of protection settings based on the operating conditions of the network. For example, protection settings can be dynamically modified based on the level of DER penetration, load conditions, and network topology. This adaptability ensures that protection devices remain effective even as network conditions change. Effective coordination of inverter-based protection also relies heavily on communication infrastructure.

High-speed, reliable communication systems are necessary to facilitate the exchange of information between various protection devices and control centers. This enables centralized protection schemes, where protection settings can be coordinated and adjusted in real-time to respond to faults more effectively. The integration of communication and smart grid technologies, coupled with optimization algorithms, is revolutionizing the management and operation of modern power systems. As the electric grid evolves into a more complex, decentralized, and dynamic network, these advancements are essential for enhancing efficiency, reliability, and sustainability [8-10].

Smart grid technologies encompass a wide range of innovations that enable two-way communication between utilities and consumers, as well as within various components of the grid itself. Key technologies include Advanced Metering Infrastructure (AMI), distribution automation, demand response systems, and grid-edge devices such as smart meters and sensors. These technologies facilitate real-time monitoring and control, allowing for more responsive and adaptive grid management. High-speed and reliable communication networks are fundamental to the smart grid. These networks support the rapid exchange of data necessary for monitoring grid conditions, coordinating Distributed Energy Resources (DERs), and implementing automated control actions.

Communication protocols such as IEC 61850, IEEE 802.11, and cellular networks are commonly used to ensure seamless data flow and interoperability among diverse grid components. Optimization algorithms play a critical role in managing the complex operations of smart grids. These algorithms are designed to solve various challenges, such as load balancing, voltage regulation, fault detection, and energy scheduling. By leveraging data from smart grid technologies, optimization algorithms can enhance the decision-making process, leading to improved grid performance.

Advanced optimization techniques, including linear programming, mixed-integer programming, genetic algorithms, and machine learning, are employed to address specific grid issues. For instance, optimization algorithms can dynamically allocate resources to balance supply and demand, minimize energy losses, and maximize the integration of renewable energy sources. The synergy between

communication technologies and optimization algorithms driving the transition towards more intelligent and resilient power systems. Future developments are expected to focus on enhancing the scalability and robustness of these systems, integrating more advanced AI and machine learning techniques, and ensuring cybersecurity in an increasingly digital grid environment [11-14].

Optimizing relay coordination in radial distribution systems with significant solar PV integration presents several challenges and problems. These issues stem from the unique operational characteristics of PV systems and the variability they introduce into the grid. Solar PV systems are inherently variable and intermittent, producing power that fluctuates with weather conditions and time of day. This variability affects the fault current levels and overall load profiles, complicating the relay coordination process.

Traditional relay settings may not be effective under these fluctuating conditions, leading to potential miscoordination and reduced protection reliability. PV inverters contribute significantly lower fault currents compared to conventional synchronous generators. This low fault current can hinder the operation of traditional overcurrent protection devices, which rely on high fault currents for accurate fault detection and isolation.

The reduced fault current levels challenge the sensitivity and selectivity of existing protection schemes, necessitating the development of new methods to ensure reliable fault detection. The integration of PV systems can introduce bidirectional power flow in radial distribution systems, especially when PV generation exceeds local load demand. This bidirectional flow complicates the relay coordination process, as protection devices must now account for faults in both forward and reverse power flow conditions.

Traditional protection schemes designed for unidirectional flow may fail to provide adequate protection under these new conditions [15-17]. PV systems can cause unintentional islanding, where a portion of the grid continues to be powered by local PV sources even after disconnection from the main grid. Detecting and mitigating islanding conditions is critical for maintaining safety and reliability.

However, traditional protection schemes may struggle with reliable islanding detection, leading to potential safety hazards and operational issues. Integrating PV systems into existing distribution networks requires careful coordination with pre-existing protection devices.

Ensuring that new relay settings do not interfere with or compromise the operation of existing devices is a complex task. It requires a thorough understanding of the entire protection scheme and may involve significant reconfiguration and testing [17-20]. The following objectives

are considered for implementing relay coordination in radial distribution systems with solar PV integration:

- Relay coordination strategies are developed to enhance protection mechanisms, ensuring efficient fault detection and isolation in radial distribution systems with integrated solar PV.
- Relay coordination schemes are designed and evaluated to effectively manage the challenges posed by the intermittent and bidirectional power flow characteristics of solar PV systems.
- Key relay parameters, such as currents and time multiplier settings, are investigated and optimized to maintain system stability and minimize outage risks in the presence of solar PV.
- The IEEE-13 bus system is used as a testbed to simulate and assess the effectiveness of the proposed relay coordination strategies under various operating conditions.
- Mi-Power software is employed for rigorous validation and analysis of the coordination schemes, ensuring their robustness and reliability in real-world scenarios.
- The specific complexities introduced by solar PV systems, such as intermittent generation and bidirectional power flows, are identified and addressed to develop comprehensive solutions for modern distribution networks.

## 2. Mathematical Modelling

### 2.1. Radial Distribution Model

The onward and reverse sweep method is used in Radial Distribution Systems (RDS) to determine load flows. Consequently, the power for the RDS is calculated. The total power in the Radial Distribution System is represented by the following Equation (1),

$$C = (A_i + jB_i) \quad i = 1 \text{ to } n \quad (1)$$

$A_i$ ,  $B_i$ , and  $C_i$  are real, reactive, and complex powers on the bus.

Reverse Sweep can be expressed in the following expression (2),

$$I_j^{(K)} = \frac{(A_j + B_j)}{V_j^{(K-1)}} \quad (2)$$

Where  $I_{ij}^{\{k\}} = I_j^{(k)}$  + all the currents of branches derived from bus N.

Onward Sweep can be expressed in Equation (3),

$$V_j^{(k)} = V_j^{(k)} - Z_{ij}^{(k)} * I_{ij}^{(k)} \quad (3)$$

Where  $j= 2$  to  $N$ ,  $i= 1$  to  $N-1$ ,  $K=1$  to  $N$ .

### 2.2. IDMT Relay

The operational time of an Inverse Definite Minimum Time (IDMT) relay varies inversely with the magnitude of the fault current relative to a predetermined threshold. When the fault current surpasses this threshold, the relay's operating time stabilizes at a slightly higher level.

Specific formulas grounded in these principles govern the determination of the IDMT relay's operation time. This ensures that the relay responds promptly to faults when the fault current is high while maintaining stability and reliability by stabilizing its response once the fault current exceeds the preset threshold [1],

$I_R$  refers to the current that flows through the protective relays when they are activated during a fault condition, as expressed in Equation (4),

$$I_R = \frac{I_f}{CR \text{ Ratio}} \quad (4)$$

Pick up current can be expressed as expression 5,

$$PC \text{ (pick up current)} = \text{at secondary of C.T} * \text{current setting (rated)} \quad (5)$$

Operating time has been expressed in the following expression (6),

$$T = \frac{k}{I_R^{\alpha} - 1} * TMS \quad (6)$$

Table 1. Significant parameters of the distribution system

| S. No. | Curve Type  | Alpha | k    |
|--------|-------------|-------|------|
| 1      | Model Curve | 0.03  | 0.2  |
| 2      | Inverse     | 1.1   | 12.3 |
| 3      | High        | 3.0   | 90   |
| 4      | Extra time  | 1.1   | 123  |

The fundamental structure of a relay, as depicted in Figure 1, comprises essential components such as a coil, core, contacts, and a mechanical assembly. When energized by a control signal, the coil creates a magnetic field, which attracts the core, causing a mechanical movement that closes or opens the contacts, thereby completing or interrupting the circuit. This operation enables the relay to perform its intended function, whether it be protecting electrical systems from faults, controlling the flow of power, or performing other automated tasks based on predetermined conditions.

The fault current for IDMT protection is computed using the system's full load current at a chosen MVA. First, the transformer's maximum through-fault current at the secondary is determined. Next, the current pick-up value at the rated MVA is selected. Based on the requirements, an appropriate

IDMT curve is chosen. Subsequently, the total load current at the selected MVA base is calculated. Finally, the PMS (Protection Management System) plug setup calculation is performed. Each of these steps ensures the precise and reliable functioning of the IDMT protection system, thereby safeguarding the electrical system from faults.

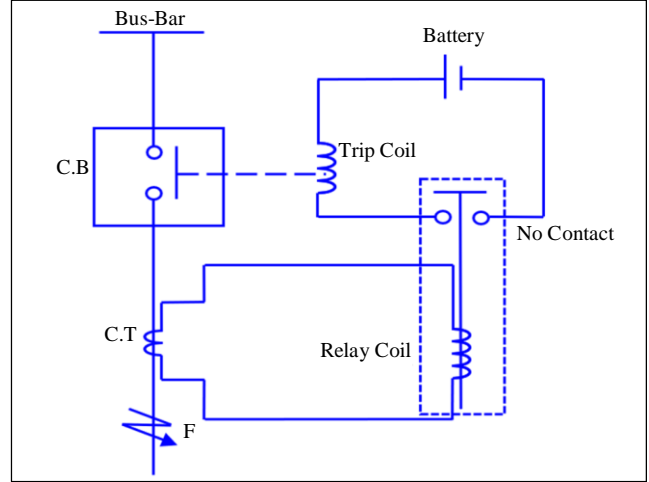


Fig. 1 Fundamental structure of relay coil circuit

By following these criteria, the PMS settings are optimized to respond accurately to variations in load and fault conditions, enhancing the overall stability and safety of the power system. The meticulous determination of the maximum through-fault current and the careful selection of the pick-up value and IDMT curve are crucial in achieving an efficient protection strategy. The comprehensive calculation of the total load current ensures that the protection system is tuned correctly, providing robust defense against electrical faults.

The current pick-up value is decided upon first. The preferred tripping time ( $T_d$ ) is then chosen, and the Plug Setting Multiplier (PSM) is set according to the fault current. To compute the relay operation time at the determined PSM, the Time Multiplier Setting (TMS) is utilized. Finally, the necessary desired trip time required by the TMS is determined. This process ensures that the relay operates correctly by adjusting the settings based on the fault current and the desired tripping time.

The TMS calculation is crucial for achieving accurate and timely relay operation, protecting electrical systems by preventing damage and ensuring safety. Each step in this procedure is essential for the proper functioning of the relay, starting from deciding the pick-up value, setting the PSM, using TMS for time computation, and determining the desired trip time. The entire process is meticulously followed to maintain the reliability and effectiveness of the relay system, ensuring that it responds appropriately to faults and protects the electrical infrastructure from potential hazards. Significant parameters of the distribution system are represented in Table 1.

### 2.3. IDMT Relay Coordination

This system is designed to address issues in power systems as quickly as possible. The amount of electricity flowing through the system is considered, and actions to rectify the fault are determined accordingly. To ensure that the system functions as intended, the relay system must be correctly configured. This involves setting the appropriate timing and power levels for each relay, which enhances the efficiency of the system. Figure 2 illustrates the relay characteristics during fault current conditions.

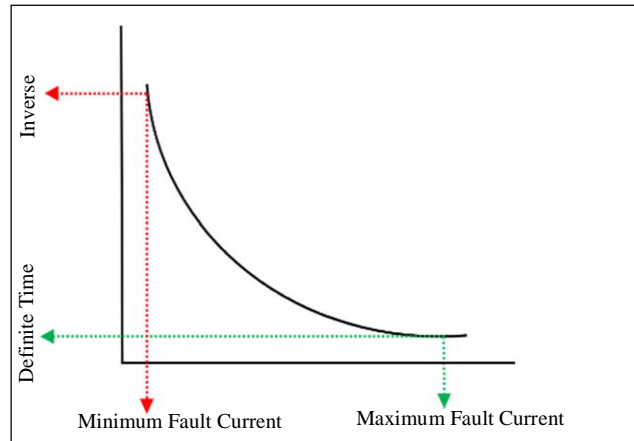


Fig. 2 Relay characteristics

Various reasons can lead to the failure of primary protection, such as power loss, issues with the relay's power, circuit breaker problems, or faults within the main protective relays. The correct setup of the relay system is essential for its proper operation. Initially, the current pick-up value is determined. Next, the preferred tripping time is chosen, and the PSM is adjusted based on the fault current.

The TMS is then used to calculate the relay operation time at the determined PSM. The desired trip time required by the TMS is subsequently established. This structured approach ensures that the relay operates correctly by adjusting the settings according to the fault current and the desired tripping time. Each step in this procedure is critical for maintaining the reliability and effectiveness of the relay system. The entire process, from deciding the pick-up value to setting the PSM, utilizing the TMS for time computation, and determining the desired trip time, is meticulously followed to ensure the relay system responds appropriately to faults. This response helps protect the electrical infrastructure from potential hazards, thereby enhancing safety and preventing damage.

Primary protection is designed to detect and isolate faults within a specific section of the power system swiftly. It operates with a high degree of sensitivity and accuracy, ensuring that faults are cleared almost immediately. If primary protection fails to operate due to any reason, such as relay

The goal is to coordinate the relays in such a manner that the faulty section of the power system is cleared as swiftly as possible, regardless of whether the power system is arranged in a straight line or within a more complex network. Primary and backup protection are critical components of this system, providing rapid responses to issues within electrical circuits. Backup protection can utilize the same devices as primary protection or different ones, although they are generally less sensitive and cover a smaller area.

power issues or circuit breaker malfunctions, backup protection is activated. Backup protection, although less sensitive, provides an additional layer of security by covering a broader area and ensuring that faults are addressed even if the primary protection fails.

Backup protection operates using either the same devices as primary protection or separate ones, which are configured to respond when primary protection does not function. The role of backup protection is crucial, as it ensures continuity and reliability in the event of primary protection failure. By covering a broader area, backup protection ensures that any faults not addressed by primary protection are still isolated and managed, thereby safeguarding the power system.

### 2.4. Relay Coordination Methods

In time discrimination, relays are configured to respond at different times during a fault. The relay closest to the fault is intended to react first, minimizing the impact on the rest of the system. The reaction times of each relay are compared to determine which one responds the fastest.

By staggering the response times, only the relay nearest to the fault should operate initially, allowing for more precise isolation of the issue. This approach ensures that faults are managed efficiently, reducing unnecessary disruptions to the power system.

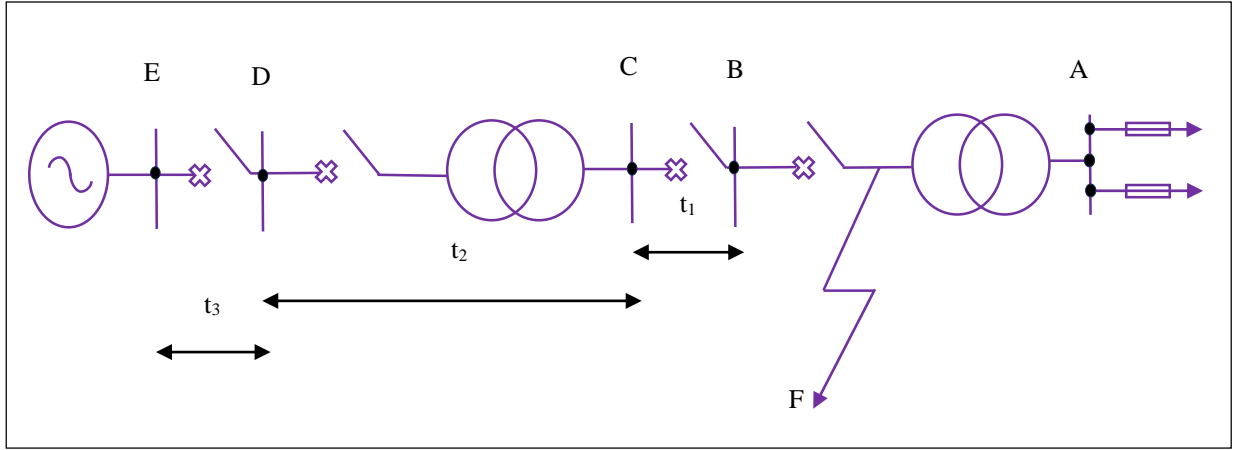


Fig. 3 Relay's operation when a problem occurs at point F

In the power system, overcurrent protection devices are installed at points B, C, D, and E. If a problem occurs at point F, the device at point B is designed to operate the quickest. If the device at B is unable to resolve the issue promptly, the device at point C will take over. This process is depicted in Figure 3.

However, if relay B does not resolve the fault within the designated timeframe, relay C acts as a backup relay. The time discrimination process is illustrated in Figure 4. By coordinating the response times of these relays, the system ensures that faults are managed efficiently, with the closest relay to the fault responding first and backup relays providing additional protection if necessary. This method minimizes disruptions and maintains the smooth operation of the power system. Current discrimination relies on fault data, as fault currents vary depending on the fault locations due to differences in resistance between the power supply and the faulty section. The relays controlling the circuit breakers are set to operate at specific threshold current levels, ensuring the nearest relay triggers its associated breaker.

Figure 5 illustrates IDMT relays coordination characteristics. This method ensures efficient fault isolation by activating the relay closest to the fault, thereby maintaining

the stability and smooth operation of the power system. This feature allows actual settings to be applied to both the current and time parameters, with the operational time being inversely correlated with the current level.

When the fault current varies significantly between the two ends of the feeder, relays located near the power source achieve faster operating times where the fault level is highest. The process begins by selecting the appropriate settings for each relay based on the current settings of adjacent relays. By configuring relays in this manner, the system ensures that those closest to the highest fault current operate first, thereby minimizing the impact on the rest of the system.

This approach allows for precise fault isolation and efficient management of the power system. The relays' settings are meticulously adjusted to account for variations in fault current, ensuring that each relay responds optimally to its specific conditions.

As a result, the overall system remains stable and operational, even in the presence of faults. This method enhances the reliability and effectiveness of the protection system, ensuring rapid response times and minimizing disruptions.

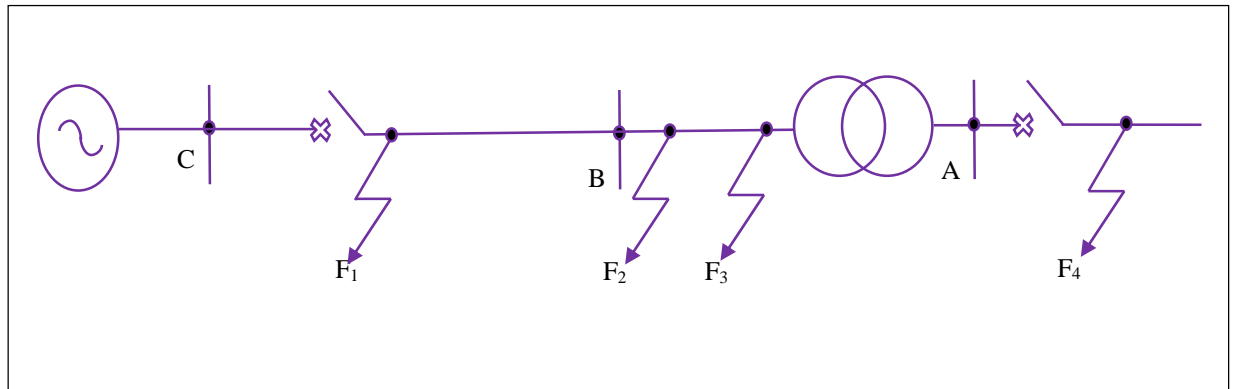


Fig. 4 Relay's operation (when C acts as a backup relay)

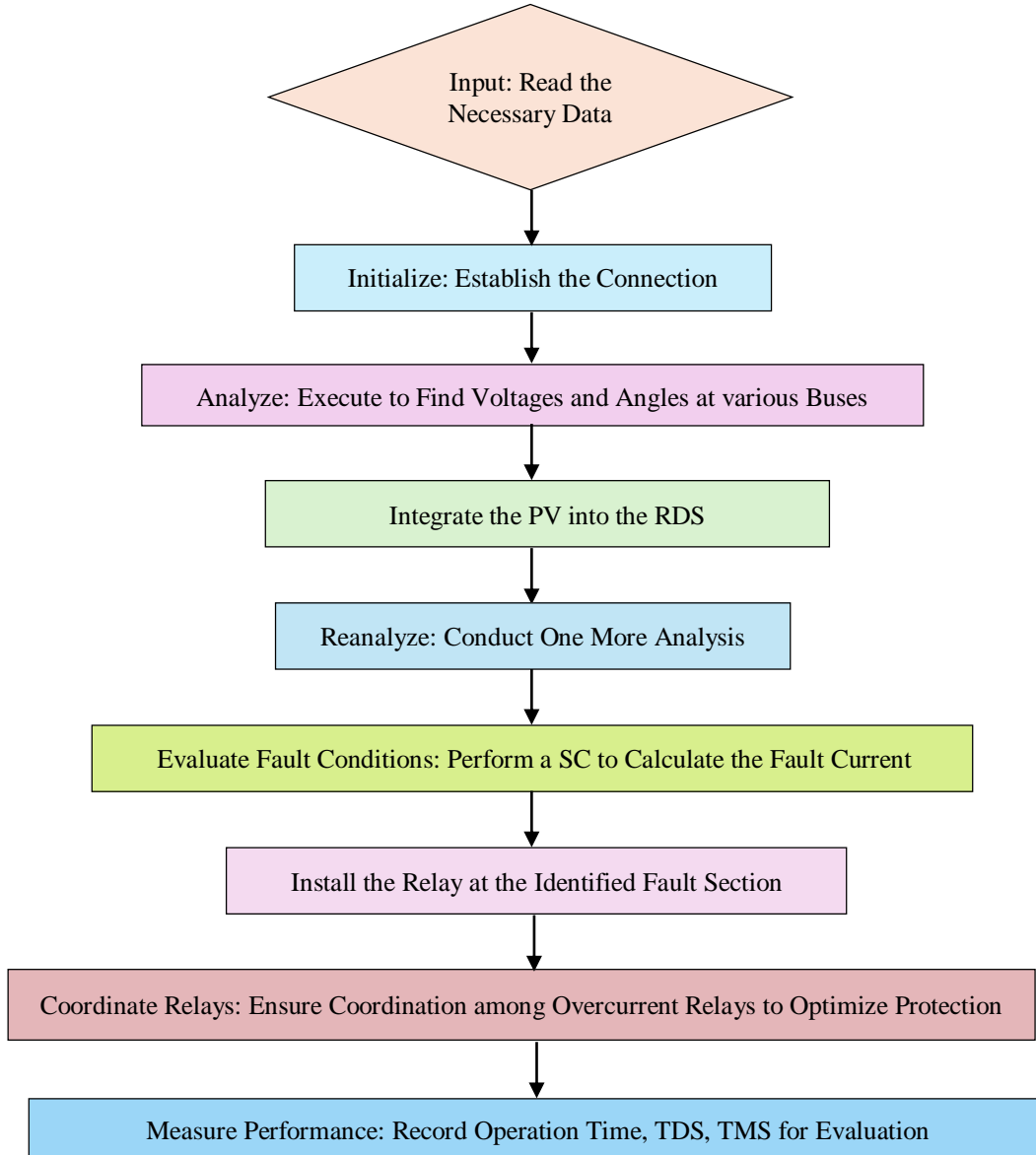


Fig. 5 IDMT relays coordinate using time-current curves

### 3. Optimal Relay Setting in Solar Photo-Voltaic Integrated 13-Bus Systems

#### 3.1. Problem Formulation

Optimizing relay settings in a solar PV integrated 13-bus system entails decreasing fault detection and isolation times while preserving system stability and protection. The constraints include system voltage restrictions, current carrying capability, coordination time intervals, and fault current levels.

The objective function tries to reduce total relay operation time while maintaining sensitivity and selectivity. Methods like optimization algorithms and modeling tools are used to establish the ideal settings, which improve system dependability and efficiency in the context of changing solar

PV production. Figure 6 illustrates the overcurrent delay test system with different parameters.

#### 3.2. Simulation Model of Solar Photo-Voltaic Integrated 13-Bus Systems

The simulation model of a solar photovoltaic-integrated 13-bus system, depicted in Figure 7, illustrates the IDMT relay coordination within a radial distribution network, including the solar system. In this configuration, 12 relays are programmed to respond progressively to failures.

Relays R5, R8, R9, R11, and R12 at the system's end perform customized main protective operations in Mi power simulation. The additional relays adapt dynamically based on the Time Multiplier Setting (TMS) and the Plug Setting



Multiplier (PSM). Relays R1, R2, R3, and R4 are coordinated with all other relays, ensuring comprehensive protection across the system. Similarly, relays R6, R7, and R10 are coordinated with relays R8, R9, R11, and R12, depending on the location of the faulted bus. These relays offer both primary

and backup protection, enhancing the reliability and safety of the distribution network. The careful coordination between these relays ensures that the system can effectively isolate faults and minimize disruption, maintaining a stable and secure power supply from the integrated photovoltaic sources.

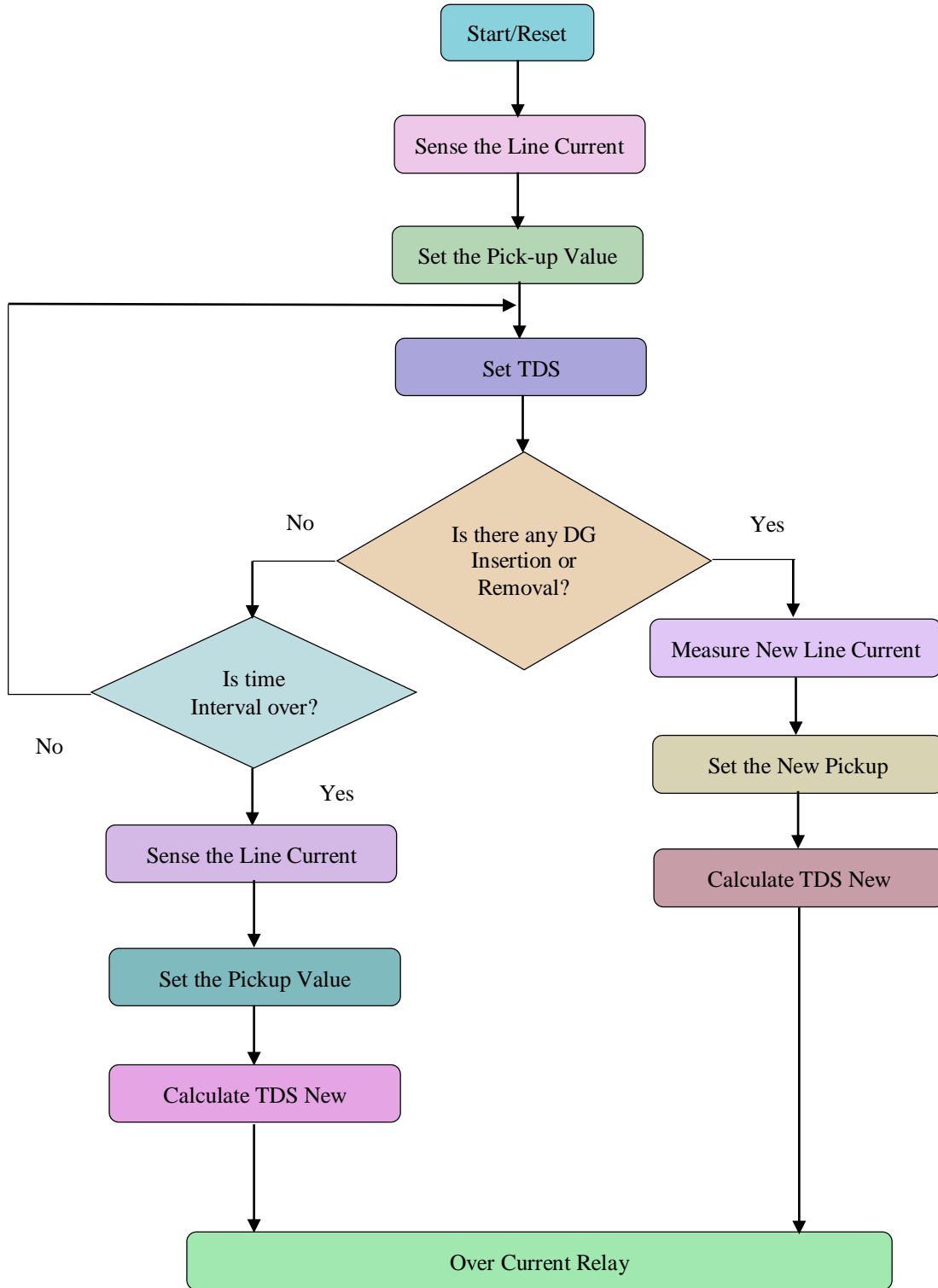


Fig. 6 Overcurrent delay test system with different parameters



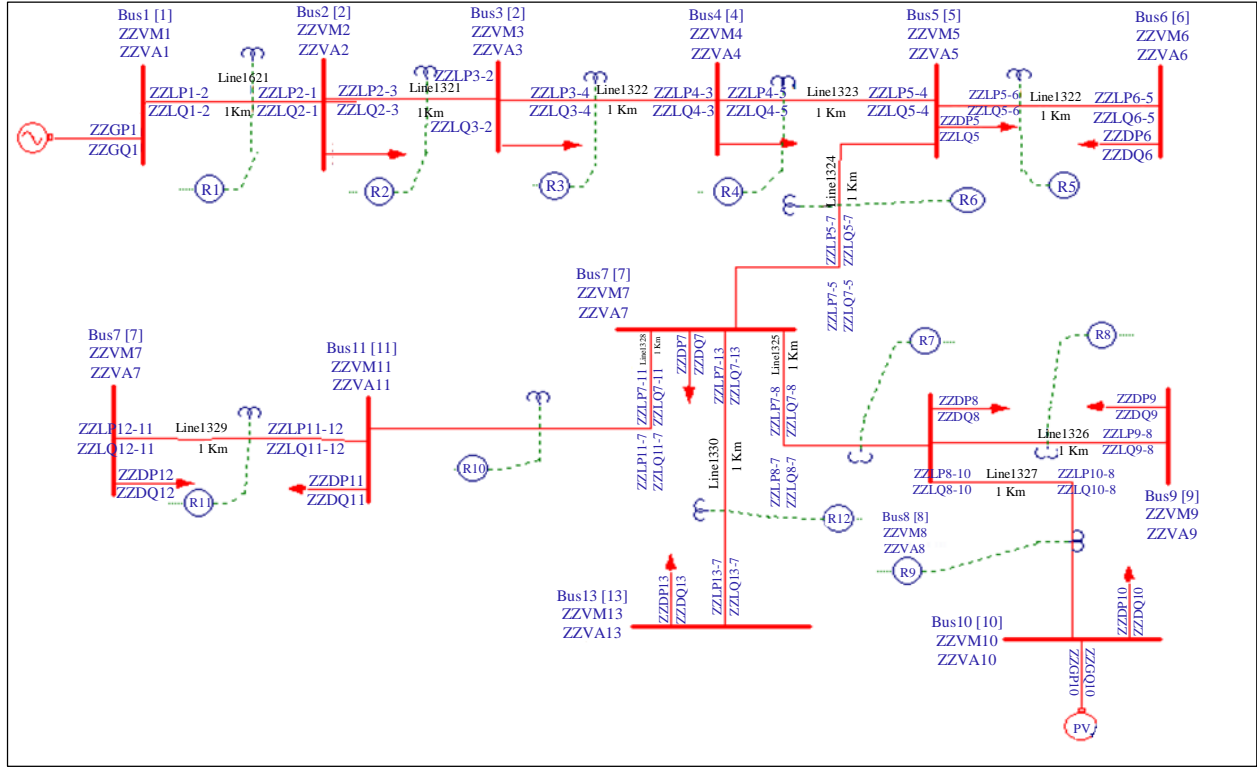


Fig. 7 IDMT relay co-ordination of RDS with solar system

### 3.3. Optimization Technique for Relay Coordination

Initially, the simulation model is coupled in order to mimic operating conditions accurately. A load flow investigation subsequently takes place to verify that electricity is distributed efficiently across the network. Short circuit analysis is then used to precisely measure fault currents, which are critical for calculating protective relay settings. IDMT overcurrent relays are strategically positioned based on the fault areas found.

Overcurrent relays are rigorously coordinated to ensure that their answers are properly sequenced. Significant variables such as operation duration, duration dial setting, time multiplier setting, and relay coordination ratio are used to fine-tune settings for effective fault prevention, and maintaining the power system's stability and safety under changing operating conditions. Table 2 illustrates the solar PV system, and Table 3 illustrates the RDS with solar Bus voltages and currents, which is used in the Mi-power simulation software tool. The following optimization procedures are carried out to incorporate an effective relay coordination system:

- Step 1: Integrate the simulation modeling.
- Step 2: Execute a load flow analysis.
- Step 3: Perform a short-circuit assessment to determine the fault current.
- Step 4: Link the IDMT overcurrent relay to the faulty component.

- Step 5: Provide the scheduling of overcurrent relays.
- Step 6: Review the operating time, time delay setting), time multiplier setting, and relay integrated ratio.

Table 2. Solar PV parameters

| S.No. | Electrical parameter                           | Quantity |
|-------|--|----------|
| 1     | DC Side Power rating (MW)                      | 0.662    |
| 2     | AC Side Power rating (MVA)                     | 0.480    |
| 3     | AC Side Voltage (kV)                           | 11       |
| 4     | No. of Inverters                               | 7        |
| 5     | Power Factor (lag)                             | 0.95     |
| 6     | Irradiance on Titled Power (w/m <sup>2</sup> ) | 1000     |
| 7     | No. of Modules in a String                     | 25       |
| 8     | No. of Strings in Array                        | 18       |
| 9     | PV Module rating (W)                           | 215      |
| 10    | Efficiency of PV Module (%)                    | 13.1     |
| 11    | Max. Power Point Voltage (V)                   | 30.2     |
| 12    | Max. PowerPoint current (A)                    | 7.13     |
| 13    | Temperature Co-efficient of Voltage (%/C)      | -0.485   |

**Table 3. RDS with solar bus voltages and currents**

| S.No. | Bus No. | RDS Without Solar | RDS With Solar |             |
|-------|---------|-------------------|----------------|-------------|
|       |         | Voltage (pu)      | Voltage (pu)   | Current (A) |
| 1     | 1       | 1.00              | 1.00           | 1102.27     |
| 2     | 2       | 0.9763            | 0.9788         | 1102.27     |
| 3     | 3       | 0.9546            | 0.9574         | 1010.09     |
| 4     | 4       | 0.9494            | 0.9526         | 935.53      |
| 5     | 5       | 0.9405            | 0.9444         | 807.28      |
| 6     | 6       | 0.9402            | 0.9441         | 56.38       |
| 7     | 7       | 0.9306            | 0.9354         | 680.117     |
| 8     | 8       | 0.9283            | 0.9336         | 193.60      |
| 9     | 9       | 0.9275            | 0.9329         | 88.95       |
| 10    | 10      | 0.9273            | 0.9334         | 25.50       |
| 11    | 11      | 0.9292            | 0.9340         | 205.97      |
| 12    | 12      | 0.9281            | 0.9329         | 136.96      |
| 13    | 13      | 0.9298            | 0.9346         | 118.81      |

Evaluating relay coordination in distribution systems with solar integration requires a systematic algorithm to ensure optimal protection and performance. The process begins with reading the necessary data, including system parameters, load profiles, and solar generation specifics. This data is essential for accurately modeling the distribution system and its behavior under various conditions. Next, establish the connection of the distribution system, ensuring all nodes, buses, and components are correctly represented.

Execute a power flow analysis to determine the voltage angles at various buses. This step is critical for understanding the baseline operation of the system and identifying potential areas of concern. Integrate the PV generation into the Radial Distribution System (RDS). This involves updating the system model to include the PV arrays, considering their locations, capacities, and generation profiles. Conduct another power flow analysis to assess the impact of the PV integration on the system's voltage profile and overall stability.

Evaluate the fault conditions by performing a Short-Circuit (SC) analysis. This analysis calculates the fault current at various points in the system, identifying the sections most vulnerable to faults. Based on this information, install relays at the identified faulted sections to provide targeted protection. Coordinate the relays to ensure optimal protection measures. This involves setting the time dial settings and time multiplier settings for each relay, ensuring that overcurrent relays operate in a coordinated manner. The goal is to optimize relay performance, minimizing the risk of unnecessary outages

while ensuring rapid isolation of faulted sections. Finally, record the operation times, TDS, and TMS for evaluation. This data is used to assess the effectiveness of the relay coordination and make any necessary adjustments.

By meticulously following this algorithm, the distribution system can be effectively protected, even with the integration of solar generation. The coordinated relay settings enhance the reliability and stability of the power system, ensuring that faults are promptly and efficiently managed. This comprehensive approach ensures that the benefits of solar integration are realized without compromising the integrity of the distribution system.

#### 4. Results and Discussion

The standard IEEE-13 radial system is considered, comprising a slack bus and 12 load buses, with a cumulative load of 12.926 MVA [13]. With a load power factor of 0.869, the system's real and reactive power demands are 10.536 MW and 6.002 MVAR, respectively. When the slack bus is connected to bus number one, the maximum current and voltage remain the same. To compute the parameters at every bus in the thirteen-bus system, forward and backward sweep techniques are used. Bus number 10 is noted for its extremely low radial distribution system voltage (0.9273). The solar photovoltaic system on this bus provides 0.662 MW of actual power and 0.218 MVAR of reactive power.

The integration of the solar system into the radial distribution grid has an impact on the grids-connected characteristics. Without the presence of the solar PV system, the Radial Distribution System (RDS) delivers 11.173 MW of traditional real power and 6.502 MVAR of reactive power for a power factor of 0.864. Whenever the Renewable Energy System (RES) at bus 10 is included, the traditional real and reactive power output of the slack bus is reduced to 10.425 MW and 6.217 MVAR, accordingly, with a power factor of 0.859. The total actual power losses in this system are 0.553282 MW and 0.433727 MVAR.

Figure 8 depicts the phase relay synchronization curves for the radial distribution system, which includes the solar PV system. The system consists of twelve relays, each strategically synchronized with others at different operating hours. Among these, relays RL5, RL8, RL9, RL11, and RL12 are designated as end relays, providing primary protection. This strategic coordination ensures efficient and reliable operation of the distribution system, even with the integration of solar generation.

Meanwhile, the time multiplier settings and plug settings of the remaining relays are dynamically adjusted over time. Notably, RL1, RL2, RL3, and RL4 are coordinated with all relays, while RL6, RL7, and RL10 are specifically coordinated with RL8, RL9, RL11, and RL12 based on the

fault bus. Integrating the RES into the distribution system prompts slight adjustments in the IDMT relay coordination characteristics and operating times. These adjustments ensure optimized relay coordination and efficient fault management within the distribution system, enhancing its reliability and performance. Relay RL1, located near the source, operates

without a backup relay. However, if RL2 is positioned closer to RL1, RL1 assumes the backup role for RL2, while RL2 functions as the primary relay. Table 4 describes the integration method for the system surviving 10 relays, which ensures appropriate distribution system security and control across a variety of failure scenarios.

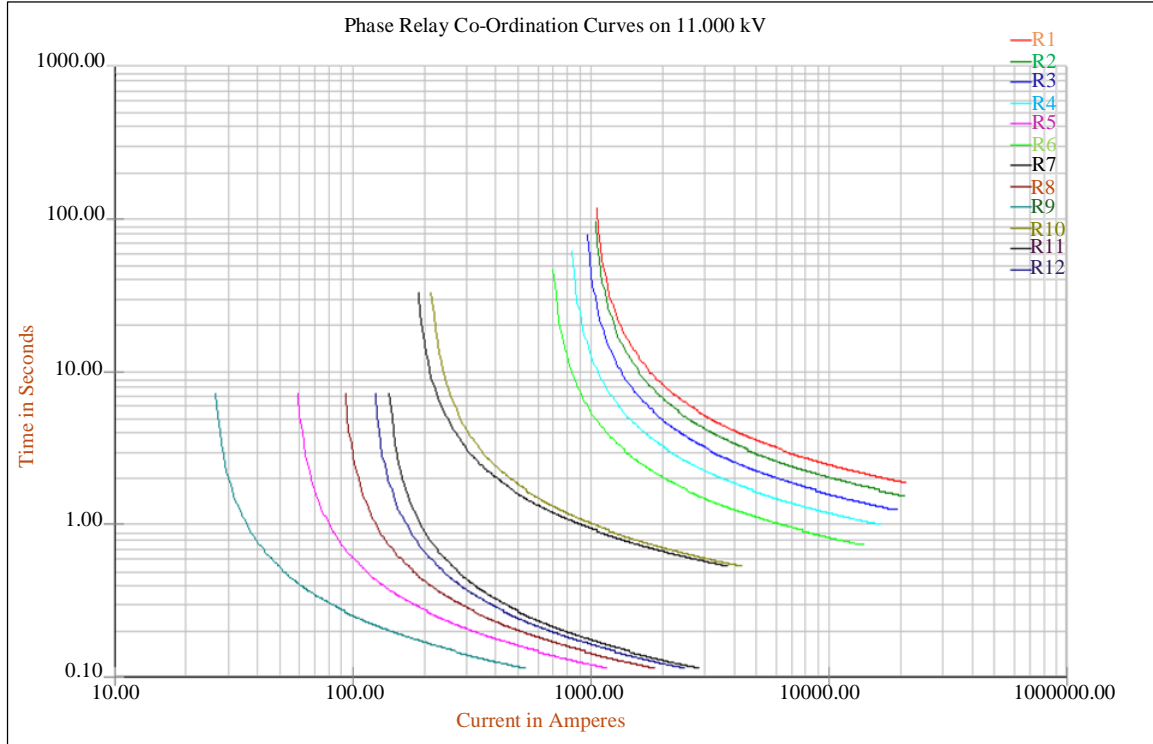


Fig. 8 IDMT relays coordination characteristics

Table 4. Potential coordinating relay in the IEEE-13 bus distribution system

| Relay Name | Co-Ordination of Relays             |
|------------|-------------------------------------|
| RL1        | NIL                                 |
| RL2        | RL1                                 |
| RL3        | RL1 - RL2                           |
| RL4        | RL1 - RL2 - RL3                     |
| RL5        | RL1 - RL2 - RL3 - RL4               |
| RL6        | RL1 - RL2 - RL3 - RL4               |
| RL7        | RL1 - RL2 - RL3 - RL4 - RL6         |
| RL8        | RL1 - RL2 - RL3 - RL4 - RL6 - RL7   |
| RL9        | RL1 - RL2 - RL3 - RL4 - RL6 - RL7   |
| RL10       | RL1 - RL2 - RL3 - RL4 - RL6         |
| RL11       | RL1 - RL2 - RL3 - RL4 - RL 6 - RL10 |
| RL12       | RL1 - RL2 - RL3 - RL4 - RL6         |

**Table 5. Operation time among coordinated relays**

| Time (s) | Main | Bac  |
|----------|------|------|
| 0.4224   | RL6  | RL4  |
| 0.4247   | RL4  | RL3  |
| 0.4251   | RL8  | RL7  |
| 0.4261   | RL9  | RL7  |
| 0.4261   | RL11 | RL10 |
| 0.4273   | RL2  | RL1  |
| 0.4375   | RL10 | RL6  |
| 0.4395   | RL3  | RL2  |
| 0.4475   | RL7  | RL6  |
| 0.8508   | RL12 | RL6  |
| 1.1206   | RL5  | RL4  |

**Table 6. Testing for phase relay integration**

| RL Name | Main | I <sub>fRB</sub> | I <sub>fRR</sub> | I <sub>fc</sub> | I <sub>frc</sub> | T.D.S |
|---------|------|------------------|------------------|-----------------|------------------|-------|
| None    | RL1  | -----            | -----            | 20281.23        | 1.8753           | 0.780 |
| RL1     | RL2  | 11971.59         | 2.2889           | 11971.61        | 1.8721           | 0.676 |
| RL2     | RL3  | 10825.22         | 1.9531           | 10824.63        | 1.5222           | 0.542 |
| RL3     | RL4  | 9091.39          | 1.6400           | 9099.01         | 1.2243           | 0.434 |
| RL4     | RL5  | 8417.62          | 1.2665           | 8417.55         | 0.1165           | 0.051 |
| RL4     | RL6  | 7521.78          | 1.3309           | 7522.11         | 0.9201           | 0.321 |
| RL6     | RL7  | 6702.43          | 0.9656           | 6702.44         | 0.535            | 0.233 |
| RL7     | RL8  | 6100.67          | 0.5311           | 6100.42         | 0.1187           | 0.056 |
| RL7     | RL9  | 5885.97          | 0.5311           | 5885.54         | 0.1188           | 0.057 |
| RL6     | RL10 | 6865.78          | 0.9557           | 6865.64         | 0.5309           | 0.232 |
| RL10    | RL11 | 6283.09          | 0.5311           | 6283.09         | 0.1134           | 0.049 |
| RL6     | RL12 | 6860.62          | 0.9565           | 6860.86         | 0.1167           | 0.048 |

When both relays RL1 and RL2 are activated, with RL2 serving as the primary relay and RL1 as the backup, they respond to the same fault current (11970.61 Amperes). However, their operating times differ; RL2, acting as the primary relay, initiates the operation, followed by RL1 as the backup after a delay. Specifically, their respective operating

times are 1.8734 seconds and 2.2897 seconds. RL2 indicates the close-in fault current, while RL1 provides the distant bus fault current.

Table 6 shows the distinct phase relay coordination inspections for the last 10 relays in the overall system. In the

event of a fault at bus number one, where the fault current reaches 20282.42 amperes, only the RL1 relay activates. Consequently, both the operating time and tripping time (1.8749 seconds) are identical. Conversely, if the fault occurs at bus number two, resulting in a fault current of 11970.61 amperes, both RL1 and RL2 relays will operate. RL2 will act

as the primary relay, triggering simultaneously with the tripping time, while RL1 functions as the backup. The backup relay's operating time will differ, occurring after the primary relay's operation. The tripping time of the backup relay will be combined with the tripping time of the adjacent relay and the operating time of the backup relay, as detailed in Table 7.

Table 7. Trip and working time of relay at fault buses

| Faulted Bus | Fault Current (A) | Name of Relay | Fault Time | Trip Time |
|-------------|-------------------|---------------|------------|-----------|
| 2           | 20198.53          | RL1           | 1.8698     | 1.8884    |
| 3           | 11897.95          | RL1           | 2.2897     | 4.1631    |
|             |                   | RL2           | 1.8734     | 1.8734    |
| 4           | 10825.15          | RL1           | 2.3906     | 5.8678    |
|             |                   | RL2           | 1.9529     | 3.4772    |
|             |                   | RL3           | 1.5243     | 1.5243    |
| 5           | 9098.96           | RL1           | 2.5875     | 7.5628    |
|             |                   | RL2           | 2.1074     | 4.9753    |
|             |                   | RL3           | 1.6408     | 2.8679    |
|             |                   | RL4           | 1.2271     | 1.2271    |
| 6           | 8417.57           | RL1           | 2.6867     | 7.9536    |
|             |                   | RL2           | 2.1848     | 5.2670    |
|             |                   | RL3           | 1.6990     | 3.0822    |
|             |                   | RL4           | 1.2679     | 1.3832    |
|             |                   | RL5           | 0.1266     | 0.1266    |
| 7           | 7499.31           | RL1           | 2.8442     | 9.1945    |
|             |                   | RL2           | 2.3073     | 6.3503    |
|             |                   | RL3           | 1.7907     | 4.0430    |
|             |                   | RL4           | 1.3318     | 2.2523    |
|             |                   | RL6           | 0.9205     | 0.9205    |
| 8           | 6702.63           | RL1           | 3.0261     | 10.2715   |
|             |                   | RL2           | 2.4481     | 7.2455    |
|             |                   | RL3           | 1.8957     | 4.7974    |
|             |                   | RL4           | 1.4045     | 2.9017    |
|             |                   | RL6           | 0.9669     | 1.4972    |
|             |                   | RL7           | 0.5303     | 0.5303    |
| 9           | 6100.83           | RL1           | 3.1926     | 10.8836   |
|             |                   | RL2           | 2.5763     | 7.6910    |
|             |                   | RL3           | 1.9909     | 5.1148    |
|             |                   | RL4           | 1.4698     | 3.1239    |
|             |                   | RL6           | 1.0084     | 1.6540    |
|             |                   | RL7           | 0.5303     | 0.6456    |
|             |                   | RL8           | 0.1153     | 0.1153    |
| 10          | 5885.86           | RL1           | 3.2610     | 11.0868   |
|             |                   | RL2           | 2.6288     | 7.8257    |
|             |                   | RL3           | 2.0297     | 5.1970    |
|             |                   | RL4           | 1.4964     | 3.1672    |
|             |                   | RL6           | 1.0252     | 1.6708    |
|             |                   | RL7           | 0.5303     | 0.6456    |
|             |                   | RL9           | 0.1153     | 0.1153    |

|    |         |      |        |         |
|----|---------|------|--------|---------|
| 11 | 6865.87 | RL1  | 2.9862 | 10.1521 |
|    |         | RL2  | 2.4173 | 7.1659  |
|    |         | RL3  | 1.8728 | 4.7486  |
|    |         | RL4  | 1.3887 | 2.8758  |
|    |         | RL6  | 0.9568 | 1.4871  |
|    |         | RL10 | 0.5303 | 0.5303  |
| 12 | 6283.18 | RL1  | 3.1385 | 10.7227 |
|    |         | RL2  | 2.5347 | 7.5842  |
|    |         | RL3  | 1.9601 | 5.0495  |
|    |         | RL4  | 1.4487 | 3.0894  |
|    |         | RL6  | 0.9950 | 1.6407  |
|    |         | RL10 | 0.5303 | 0.6456  |
|    |         | RL11 | 0.1266 | 0.1266  |
| 13 | 6798.67 | RL1  | 2.9874 | 9.7408  |
|    |         | RL2  | 2.4182 | 6.7533  |
|    |         | RL3  | 1.8735 | 4.3351  |
|    |         | RL4  | 1.3891 | 2.4616  |
|    |         | RL6  | 0.9571 | 1.0724  |
|    |         | RL12 | 0.1153 | 0.1153  |

**Table 8. Time multiplier settings and relay coordination**

| RL Name | Time-Multiplier | Ratio   |
|---------|-----------------|---------|
| RL1     | 0.789           | 17.976  |
| RL2     | 0.669           | 12.102  |
| RL3     | 0.539           | 11.546  |
| RL4     | 0.427           | 11.261  |
| RL5     | 0.051           | 149.109 |
| RL6     | 0.318           | 11.039  |
| RL7     | 0.240           | 34.582  |
| RL8     | 0.049           | 68.511  |
| RL9     | 0.049           | 230.823 |
| RL10    | 0.229           | 33.287  |
| RL11    | 0.049           | 45.822  |
| RL12    | 0.049           | 57.676  |

In this scenario, only the end relays provide primary protection, maintaining a fixed Time Multiplier Setting (TMS) value of 0.05 seconds, as specified by user functions. The remaining relays act as backups, with their TMS values adjusted dynamically. Updated values can be found in Table 8. Notably, the coordination ratio of overcurrent relay RL9 is significantly high (230.823) compared to other relays. This is attributed to the integration of a Renewable Energy Source (RES) into the radial distribution system at the 10th bus, resulting in reduced line flow currents. Specifically, the line flow currents decrease to 26 Amps between the 9th and 10th

buses, with relay R9 positioned in between. Consequently, during a fault at bus number 10, RL9's coordination ratio is notably high due to the fault current exceeding its operational fault current. At the outset, the coordination fault current between relays RL1 and RL9 stands at 26.88 Amps, progressively escalating to a final fault current of 529.09 Amps. Throughout this duration, these relays synchronize their operations. Notably, during periods of minimal fault currents, their operating times are maximized, whereas during instances of peak fault currents, relay operating times are minimized, as depicted in Figure 9.

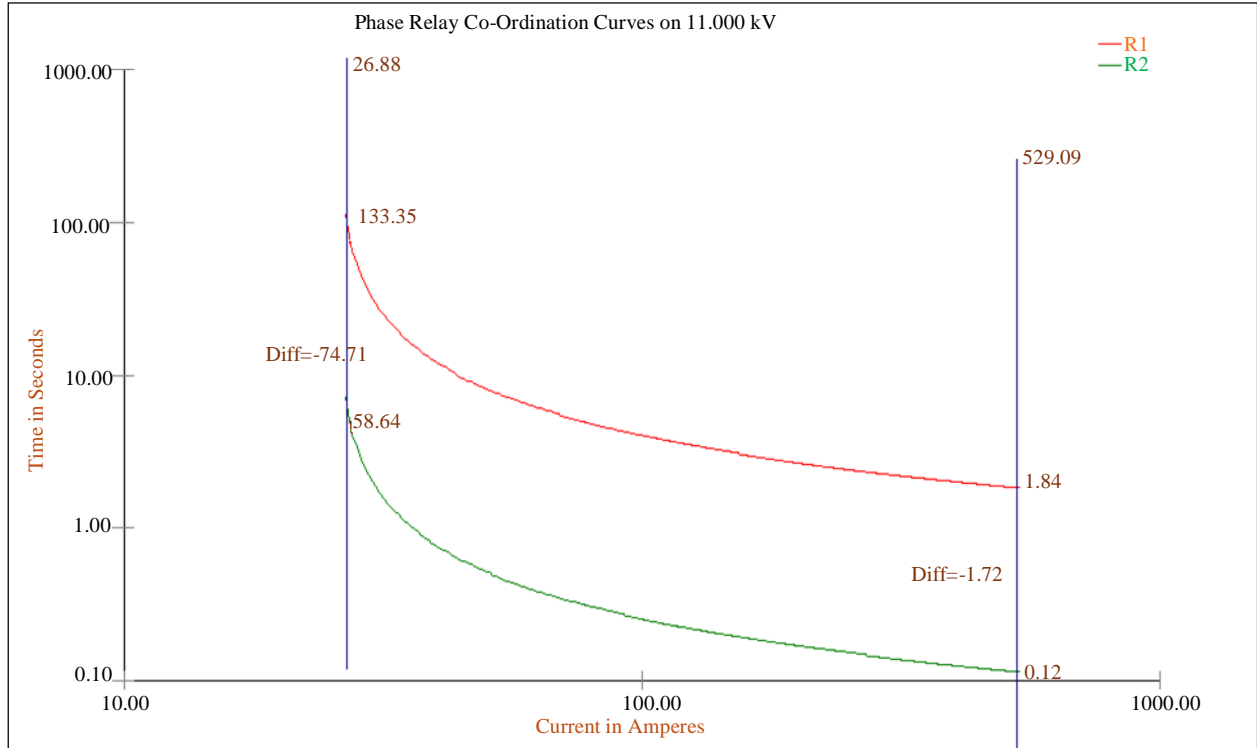


Fig. 9 R1 and R9 coordination characteristics

## 5. Conclusion

This research underscores the significance of relay coordination in radial distribution networks for the seamless integration of solar Photovoltaic (PV) systems. By optimizing both primary and backup relay coordination, the research endeavors to enhance system security and facilitate the efficient assimilation of renewable energy sources. Utilizing the IEEE-13 bus system as a testing ground, various relay coordination strategies were investigated, considering pivotal factors such as currents and time multiplier settings to formulate an effective coordination scheme. The integration

of solar PV systems introduces complexity due to bidirectional power flow and intermittent generation, necessitating sophisticated coordination techniques. Through validation using Mi-Power software, the proposed coordination strategies were assessed for their efficacy in upholding system stability and mitigating outage risks. In essence, the findings contribute to the development of tailored relay coordination methodologies for contemporary distribution networks incorporating renewable energy, thereby optimizing system performance and reliability while addressing pertinent challenges.

## References

- [1] Emilio Ghiani, and Fabrizio Pilo, "Smart Inverter Operation in Distribution Networks with High Penetration of Photovoltaic Systems," *Journal of Modern Power Systems and Clean Energy*, vol. 3, no. 4, pp. 504-511, 2015. [CrossRef] [Google Scholar] [Publisher Link]
- [2] Ángel Molina-García et al., "Reactive Power Flow Control for PV Inverters Voltage Support in LV Distribution Networks," *IEEE Transactions on Smart Grid*, vol. 8, no. 1, pp. 447-456, 2017. [CrossRef] [Google Scholar] [Publisher Link]
- [3] Eyad S. Oda et al., "Stochastic Optimal Planning of Distribution System Considering Integrated Photovoltaic-Based DG and DSTATCOM Under Uncertainties of Loads and Solar Irradiance," *IEEE Access*, vol. 9, pp. 26541-26555, 2021. [CrossRef] [Google Scholar] [Publisher Link]
- [4] Subho Paul, and Narayana Prasad Padhy, "Real-Time Advanced Energy-Efficient Management of an Active Radial Distribution Network," *IEEE Systems Journal*, vol. 16, no. 3, pp. 3602-3612, 2022. [CrossRef] [Google Scholar] [Publisher Link]
- [5] Nursyarizal Mohd Nor et al., "Battery Storage for the Utility-Scale Distributed Photovoltaic Generations," *IEEE Access*, vol. 6, pp. 1137-1154, 2018. [CrossRef] [Google Scholar] [Publisher Link]
- [6] Sérgio F. Santos et al., "New Multi-Stage and Stochastic Mathematical Model for Maximizing RES Hosting Capacity-Part II: Numerical Results," *IEEE Transactions on Sustainable Energy*, vol. 8, no. 1, pp. 320-330, 2017. [CrossRef] [Google Scholar] [Publisher Link]
- [7] Mohammad Zain Ul Abideen et al., "An Enhanced Approach for Solar PV Hosting Capacity Analysis in Distribution Networks," *IEEE Access*, vol. 10, pp. 120563-120577, 2022. [CrossRef] [Google Scholar] [Publisher Link]



- [8] Kartika Dubey, and Premalata Jena, "Novel Fault Detection & Classification Index for Active Distribution Network Using Differential Components," *IEEE Transactions on Industry Applications*, vol. 60, no. 3, pp. 4530-4540, 2024. [[CrossRef](#)] [[Google Scholar](#)] [[Publisher Link](#)]
- [9] Parimalasundar Ezhilvannan et al., "Analysis of the Effectiveness of a Two-Stage Three-Phase Grid Connected Inverter for Photovoltaic Applications," *Journal of Solar Energy Research*, vol. 8, no. 2, pp. 1471-1483, 2023. [[CrossRef](#)] [[Google Scholar](#)] [[Publisher Link](#)]
- [10] Shadab Murshid, and Bhim Singh, "A Multiobjective GI-Based Control for Effective Operation of PV Pumping System Under Abnormal Grid Conditions," *IEEE Transactions on Industrial Informatics*, vol. 16, no. 11, pp. 6880-6891, 2020. [[CrossRef](#)] [[Google Scholar](#)] [[Publisher Link](#)]
- [11] Vineeth Vijayan et al., "A Blended Approach to Improve Reliability and Efficiency of Active EDN via Dynamic Feeder Reconfiguration, Demand Response, and VVO," *IEEE Transactions on Automation Science and Engineering*, vol. 21, no. 1, pp. 684-695, Jan. 2024. [[CrossRef](#)] [[Google Scholar](#)] [[Publisher Link](#)]
- [12] Senthamizh Selvan Sakthivel et al., "Detection, Classification, and Location of Open-Circuit and Short-Circuit Faults in Solar Photovoltaic Array: An Approach Using Single Sensor," *IEEE Journal of Photovoltaics*, vol. 13, no. 6, pp. 986-990, 2023. [[CrossRef](#)] [[Google Scholar](#)] [[Publisher Link](#)]
- [13] Priyanka Mishra, Ashok Kumar Pradhan, and Prabodh Bajpai, "Time-Domain Directional Relaying Using only Fault Current for Distribution System with PV Plant," *IEEE Transactions on Power Delivery*, vol. 37, no. 4, pp. 2867-2874, 2022. [[CrossRef](#)] [[Google Scholar](#)] [[Publisher Link](#)]
- [14] Neelesh Yadav, and Narsa Reddy Tummuru, "Short-Circuit Fault Detection and Isolation Using Filter Capacitor Current Signature in Low-Voltage DC Microgrid Applications," *IEEE Transactions on Industrial Electronics*, vol. 69, no. 8, pp. 8491-8500, 2022. [[CrossRef](#)] [[Google Scholar](#)] [[Publisher Link](#)]
- [15] Luyu Wang et al., "Indirect Coordinated Attack Against Relay via Load-Side Power Electronics and Its Defense Strategy," *IEEE Transactions on Industrial Informatics*, vol. 20, no. 4, pp. 5112-5124, 2024. [[CrossRef](#)] [[Google Scholar](#)] [[Publisher Link](#)]
- [16] B. Perumal et al., "Fault analysis in the 5-level multilevel NCA DC-AC converter," *Automatika*, vol. 64, no. 3, pp. 606-612, 2023. [[CrossRef](#)] [[Google Scholar](#)] [[Publisher Link](#)]
- [17] Kartika Dubey, and Premalata Jena, "Novel Fault Detection & Classification Index for Active Distribution Network Using Differential Components," *IEEE Transactions on Industry Applications*, vol. 60, no. 3, pp. 4530-4540, 2024. [[CrossRef](#)] [[Google Scholar](#)] [[Publisher Link](#)]
- [18] Arghadeep Chowdhury et al., "Nonunit Protection of Parallel Lines Connecting Solar Photovoltaic Plants," *IEEE Systems Journal*, vol. 17, no. 2, pp. 2961-2970, 2023. [[CrossRef](#)] [[Google Scholar](#)] [[Publisher Link](#)]
- [19] Mohammed A. Al-Hitmi et al., "Symmetric and Asymmetric Multilevel Inverter Topologies with Reduced Device Count," *IEEE Access*, vol. 11, pp. 5231-5245, 2023. [[CrossRef](#)] [[Google Scholar](#)] [[Publisher Link](#)]
- [20] Parimalasundar Ezhilvannan, and Suresh Krishnan, "Fault Analysis and Compensation in a Five Level Multilevel DC-AC Converter," *El-Cezeri*, vol. 10, no. 1, pp. 99-108, 2023. [[CrossRef](#)] [[Google Scholar](#)] [[Publisher Link](#)]